別紙 3

D．考察

H24年度の検討でCLTは網膜神経節細胞と網膜色素上皮細胞の低酸素・低栄養負荷培養に対して、細胞保護作用およびROS産生抑制作用が示唆されている。経強膜的に徐放されたCLTが神経網膜または網膜色素上皮細胞に到達し、光障害に伴う酸化ストレス障害を抑制したことが示唆される。

この結果はCLTの網膜保護剤としての新規薬効を示しており、さらに徐放デバイス化によって、投与量を調整して全身性の副作用を抑制しながら、網膜局所の治療ができる可能性を示している。

E．結論

CLT-DDSの網膜保護剤としての可能性を示した。

F．健康危険情報

該当なし

G．研究発表

1．論文発表

1. **Nagai N**, Kaji H, Onami H, Ishikawa Y, Nishizawa M, Osumi N, Nakazawa T, Abe T. A polymeric device for controlled transscleral multi-drug delivery to the posterior segment of the eye, *Acta Biomaterialia*, **10**, 680-687, 2014.
2. **Nagai N**, Kaji H, Onami H, Katsukura Y, Ishikawa Y, Zhaleh KN, Sampei K, Iwata S, Ito S, Nishizawa M, Nakazawa T, Osumi N, Mashima Y, Abe T. A Platform for Controlled Dual-Drug Delivery to the Retina: Protective Effects against Light-Induced Retinal Damage in Rats. *Advanced Healthcare Materials*, in press, DOI:10.1002/adhm.201400114. 2014.

2．学会発表

（国際学会発表）

1. **Nagai N**, Kaji H, Onami H, Yamada T, Katsukura Y, Ishikawa Y, Nishizawa M, Mashima Y, Abe T. Protective Effects of Transscleral Drug Delivery Device Against Photoreceptor Cell Death in S334ter Rhodopsin Mutant Rats. ARVO2013 annual meeting, Seattle, Washington (May 5-9, 2013)

（国内学会発表）

1. Zhaleh KN, **Nagai N**、Yamamoto K, Saya H, Kaji H, Nishizawa M, Nakazawa T, Abe T. Protective effects of sustained clotrimazole release against light-induced retinal degeneration in rats. 第 35 回バイオマテリアル学会大会、タワーホール船堀（2013 年 11 月 25 日-26 日）
2. Zhaleh KN, **Nagai N**, Yamamoto K, Saya H. Kaji H, Nishizawa M. Nakazawa T, Abe T. Protective effects of Clotrimazole against oxidative stress-induced cell death in RGC-5 cells and preparation of controlled release device. 第 29 回日本 DDS 学会学術集会、京都テルサ（2013 年 7 月 4 日-5 日）

H．知的財産権の出願・登録状況（予定を含む。）

1. 特許取得
   なし
2. 実用新案登録
   なし
3. その他
   なし

別紙３

研究報告書

厚生労働科学研究費補助金（障害者対策総合研究事業）
（分担）研究報告書

網膜保護用デバイスの開発に関する研究

研究分担者　西澤松彦　東北大学大学院工学研究科　教授

研究要旨：
本研究は、比較的短期間で実現可能な既存薬や安全性が担保された薬剤ライブラリーを用いた神経保護薬剤スクリーニングとドラックデリバリーシステム（DDS）を確立することが目的である。分担研究として H25 年度は前年度から引き続き、将来的に人に応用するための検討として、微細加工法によるデバイス形状の最適化方法を検討した。臨床データから平均的な眼球サイズを計算し、デバイス先端が黄斑部周辺に届く長さと、眼球の曲率にあったデバイスの設計を行った。また、デバイスに複数の溝をつけることで、縫合位置を限定せずに任意の部位に縫合できるデバイス設計を行った。

A．研究目的

本研究は、比較的短期間で実現可能な既存薬や安全性が担保された薬剤ライブラリーを用いた神経保護薬剤スクリーニングとドラックデリバリーシステム（DDS）を確立することが目的である。将来的に人に応用するための検討として、微細加工法によってデバイス形状を最適化する方法を検討した。H25年度は、臨床データから平均的な眼球サイズを計算し、デバイス先端が黄斑部周辺に届く長さと、眼球の曲率にあったデバイスの設計を行った。また、デバイスに複数の溝をつけることで、縫合位置を限定せずに任意の部位に縫合できるデバイス設計を行った。

微細加工は切削装置のMicroMC-2（PMT Co.）を使用した。これはマイクロ単位でアクリル板上にCAD（Computer aided design）でデザインした設計図を切削することができる。デバイスの形状をCADで作製し、アクリル板に掘って鋳型を作製し、これをもとにPDMS（ポリジメチルシロキサン）に鋳型を転写し、この2次鋳型を用いて、DDSの基材であるPEGDM(ポリエチレングリコールジメタクリレート)を光重合し、デバイスを作製している。

B．研究方法

１．デバイス作製用PDMS鋳型の作製

CAD(computer assisted drawing)で鋳型の設計図を作成し、それを「小型NC微細加工機Micro MC-2(株式会社PMT)」へ取り込み、CAMによってボールエンドミルを使用してアクリル樹脂を切削加工した。このアクリル板にPDMSを乗せ、60℃でPDMSを硬化し、リザーバー形状をPDMSに転写した。

このPDMSをシラン化処理した。以下、シラン化処理を示す。PDMSをエタノール、蒸留水の順で10分間ずつ超音波洗浄し、オーブンで乾燥した。プラズマアッシャー（YHS-R）で30秒間酸素プラズマ処理を施した。プラズマ処理したPDMSをシャーレに置き、ドラフト内でシラン（1H,1H,2H,2H-PERFLUOROOCTYLTRICHLOROSILANE、WAKO）を2ヶ所に2 μlずつPDMSに付かないように垂らし、ふたをして１時間以上静置した。

シラン化処理したPDMS上に別のPDMSを乗せて、60℃で硬化した。このPDMS鋳型が最終形である。

２．デバイス（リザーバー）の作製

PDMS鋳型に、Triethyleneglycoldimethacrylate（TEGDM、Adrich）5mLに2-Hydroxy-2-methyl-propiophenoneを0.1mL混合したプレポリマーを流し、UV架橋（11.6mW/cm2、40秒、LC8、浜松ホトニクス）してリザーバーを作製した。このPDMSをシラン化処理した。以下、シラン化処理を示す。PDMSをエタノール、蒸留水の順で10分間ずつ超音波洗浄し、オーブンで乾燥した。プラズマアッシャー（YHS-R）で30秒間酸素プラズマ処理を施した。プラズマ処理したPDMSをシャーレに置き、ドラフト内でシラン（1H,1H,2H,2H-PERFLUOROOCTYLTRICHLOROSILANE、WAKO）を2ヶ所に2 μlずつPDMSに付かないように垂らし、ふたをして１時間以上静置した。

シラン化処理したPDMS上に別のPDMSを乗せて、60℃で硬化した。このPDMS鋳型が最終形である。

２．デバイス（リザーバー）の作製

PDMS鋳型に、Triethyleneglycoldimethacrylate（TEGDM、Adrich）5mLに2-Hydroxy-2-methyl-propiophenoneを0.1mL混合したプレポリマーを流し、UV架橋（11.6mW/cm2、40秒、LC8、浜松ホトニクス）してリザーバーを作製した。

C．研究結果

１．デバイス鋳型の作製

角膜を入れた日本人眼軸長は平均23.8mmと計算された（Fig.1）。角膜を考慮し眼球中心から黄斑までを11mm、眼球中心から赤道部までを12mmとした。赤道部から黄斑部まで計算上18mmと考えられ、赤道部から角膜輪部までは10.8mmと計算した。デバイス先端が黄斑でデバイス後端が赤道部とするとデバイスサイズは18mmとなるが、強膜に糸をかける位置とデバイスの縫合糸溝の位置などを考慮するとなるとデバイスの長さは①19mm、②21mm、③23mmの３種類が適切と判断した。臨床で使用されていた黄斑プロンベは長さが21-27mmで21mmは最短となるが、黄斑プロンベそのものが近視の網膜剥離に使用することが多いことを考慮すると妥当な値と考えた。デバイスの縫合溝がデバイス後端より1.4mmで、溝幅が0.3mmで、もうひとつの糸溝がそこから1.7mmになるので、デバイス後端から奥の縫合溝まで3.4mmになる。

眼球のカーブはこれまでのデータからまず眼球直径24mmを考えた。さらに角膜の突出、眼軸長分布、デバイスフィット状態を考慮して22mmも考慮した。したがってデバイス長①②③に対してそれぞれ24mm、22mmの円を考慮したデバイスカーブを作製することで、

平均的な成人の眼球に適応可能なデバイスが準備できると考えられる。

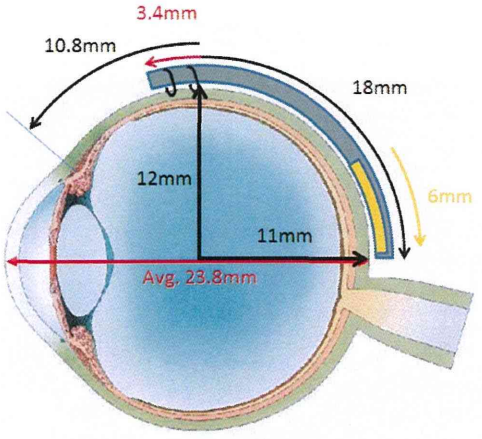

Fig.1 ヒトの平均的な眼球サイズとデバイスサイズ

２．縫合溝の形状検討

デバイスを強膜に固定するための縫合糸を引掛ける溝として、デバイス後端部に側面にそれぞれ2か所の溝を設計した（Fig.2a）。しかし、眼球モデルにデバイスの固定を検討した結果、縫合で縛る力によって後端部が強膜に押し付けられ、逆に先端側が強膜から浮いてしまう可能性が指摘された。そこで、デバイスの先端部により近い部分に複数の溝を設計した（Fig.2b）。この形状によって縫合糸を掛ける位置がよりデバイス先端側に移動するため、デバイスの浮きがありを抑制できると期待できる。また、縫合糸のかけ方に自由度が増し、状況に応じて縫合部位を変えることができる。また別のパターンとして、横に溝をつけるのではなく、デバイス上面に横一直線の溝を設計した。突起物がなくなるため、安全に縫合できる可能性がある。

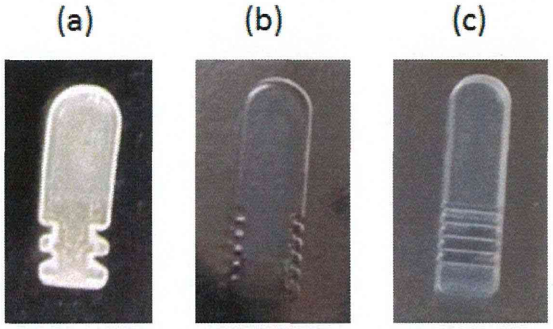

Fig.2 リザーバーの形状

D．考察

網膜疾患治療では、黄斑部周囲に薬剤を届ける必要があるため、できるだけ後眼部へデバイスのリザーバー部位を挿入する必要がある。また、徐放面が強膜に密着しなければ、Fibrosisが徐放面に侵入し薬剤が吸収されたり、デバイスと強膜の隙間から薬剤が逃げて結膜へ吸収され、薬剤送達効率が悪くなる可能性がある。今回のプロトタイプでは、縫合糸による強膜上への固定が可能となり、強膜への密着が強化された。

今後はモデルドラッグで眼内への移行性、薬物分布を評価し、移行が確認できたら、実際の薬物で網膜変性動物に移植し、治療効果を確認していく。

E．結論

ヒト眼用のデバイス形状を作成した。今後は治験用デバイスの作製のための準備をしていく。

別紙 3

F．健康危険情報

該当なし

G．研究発表

1． 論文発表

1. Nagai N, Kaji H, Hideyuki Onami, Yumi Ishikawa, **Nisizawa M**, Noriko Osumi, Toru Nakazawa, Toshiaki Abe. “A polymeric device for controlled transscleral multi-drug delivery to the posterior segment of the eye” Acta Biomaterialia, 10, 680-687 (2014).

2. Nagai N, Kaji H, Hideyuki Onami, Yuki Katsukura, Yumi Ishikawa, Zhaleh KN, Kaori Sampei, Satoru Iwata, Shuntaro Ito, **Nisizawa M**, Toru Nakazawa, Noriko Osumi, Yukihiko Mashima, Toshiaki Abe. ”A Platform for Controlled Dual-Drug Delivery to the Retina: Protective Effects against Light-Induced Retinal Damage in Rats” Advanced Healthcare Materials, in press, DOI:10.1002/adhm.201400114 (2014).

2． 学会発表

（国際学会発表）

1. Nagai N, Kaji H, Onami H, Yamada T, Katsukura Y, Ishikawa Y, **Nisizawa M**, Mashima Y, Abe T. Protective Effects of Transscleral Drug Delivery Device Against Photoreceptor Cell Death in S334ter Rhodopsin Mutant Rats. ARVO2013 annual meeting, Seattle, Washington (May 5-9, 2013)

（国内学会発表）

1. Zhaleh KN, Nagai N, Yamamoto K, Saya H, Kaji H, Nishizawa M, Nakazawa T ,Abe T. Protective effects of sustained clotrimazole release against light-induced retinal degeneration in rats. 第 35 回バイオマテリアル学会大会,タワーホール船堀（2013 年 11 月 25 日-26 日）

2. Zhaleh KN, Nagai N, Yamamoto K, Saya H, Kaji H, Nishizawa M, Nakazawa T, Abe TProtective effects of Clotrimazole against oxidative stress-induced cell death in RGC-5 cells and preparation of controlled release device. 第 29 回日本 DDS 学会学術集会、京都テルサ（2013 年 7 月 4 日-5 日）

H．知的財産権の出願・登録状況

（予定を含む。）

1. 特許取得

なし

2. 実用新案登録

なし

3.その他

なし

別紙４

研究成果の刊行に関する一覧表（阿部　俊明）

雑誌

発表者氏名	論文タイトル名	発表誌名	巻号	ページ	出版年
Nagai N, Kaji H, Onami H, Katsukura Y, Ishikawa Y, Nezhad ZK, Sampei K, Iwata S, Ito S, Nishizawa M, Nakazawa T, Osumi N, Mashima Y, Abe T	A Platform for Controlled Dual-Drug Delivery to the Retina: Protective Effects against Light-Induced Retinal Damage in Rats	Adv Healthc Mater	doi: 10.1002/adhm.201400114. [Epub ahead of print]		2014
AbeT, Tokita-Ishikawa Y, Onami H, Katsukura Y, Kaji H, Nishizawa M, Nagai N	Intrascleral Transplantation of a Collagen Sheet with Cultured Brain-Derived Neurotrophic Factor Expressing Cells Partially Rescues the Retina from Damage due to Acute High Intraocular Pressure. Retinal Degenerative Diseases	Advances in Experimental Medicine and Biology	Volume 801	837-843	2014
Nagai N, Kaji H, Onami H, Ishikawa Y, Nishizawa M, Osumi N, Nakazawa T, Abe T.	A polymeric device for controlled transscleral multi-drug delivery to the posterior segment of the eye	Acta Biomater	10	680-7	2014
Kunikata H, Aizawa N, Meguro Y, Abe T, Nakazawa T.	Combined 25-gauge microincision vitrectomy and toric intraocular lens implantation with posterior capsulotomy.	Ophthalmic Surg Lasers Imaging Retina	44	145-54	2013
Kunikata H, Yasuda M, Aizawa N, Tanaka Y, Abe T, Nakazawa T	Intraocular concentrations of cytokines and chemokines in rhegmatogenous retinal detachment and the effect of intravitreal triamcinolone acetonide	Am J Ophthalmol	155	1028-37	2013

別紙４

研究成果の刊行に関する一覧表（中澤　徹）

雑誌

発表者氏名	論文タイトル名	発表誌名	巻号	ページ	出版年
Hagiwara K, Obayashi T, Sakayori N, Yamanishi E, Hayashi R,Osumi N, Nakazawa T, Nishida K	Molecular and cellular features of murine craniofacial and trunk neural crest cells as stem cell-like cells	PLoS One	9	e84072	2014
Takahashi M, Omodaka K, Maruyama K, Yamaguchi T, Himori N, Shiga Y, Ryu M, Kunikata H, Nakazawa T.	Simulated Visual Fields Produced from Macular RNFLT Data in Patients with Glaucoma	Curr Eye Res	38	1133-1141	2013
Takahashi H, Sugiyama T, Tokushige H, Maeno T, Nakazawa T, Ikeda T, Araie M	Comparison of CCD-equipped laser speckle flowgraphy with hydrogen gas clearance method in the measurement of optic nerve head microcirculation in rabbits	Exp Eye Res	108	10-15	2013
Shiga Y, Shimura M, Asano T, Tsuda S, Yokoyama Y, Aizawa N, Omodaka K, Ryu M, Yokokura S, Takeshita T, Nakazawa T.	The influence of posture change on ocular blood flow in normal subjects, measured by laser speckle flowgraphy	Curr Eye Res	38	691-698	2013
Shi D, Takano Y, Nakazawa T, Mengkegale M, Yokokura S, Nishida K, Fuse N	Molecular genetic analysis of primary open-angle glaucoma, normal tension glaucoma, and developmental glaucoma for the VAV2 and VAV3 gene variants in Japanese subjects	Biochem Biophys Res Commun	432	509-512	2013
Shi D, Funayama T, Mashima Y, Takano Y, Shimizu A, Yamamoto K, Mengkegale M, Miyazawa A, Yasuda N, Fukuchi T, Abe H, Ideta H, Nishida K, Nakazawa T, Richards JE, Fuse N	Association of HK2 and NCK2 with normal tension glaucoma in the Japanese population	PLoS One	8	e54115	2013

別紙４

研究成果の刊行に関する一覧表（中澤　徹）

雑誌

発表者氏名	論文タイトル名	発表誌名	巻号	ページ	出版年
Omodaka K, Kunimatsu-Sanuki S, Morin R, Tsuda S, Yokoyama Y, Takahashi H, Maruyama K, Kunikata H, Nakazawa T	Development of a new strategy of visual field testing for macular dysfunction in patients with open angle glaucoma	Jpn J Ophthalmol	57	457-462	2013
Himori N, Yamamoto K, Maruyama K, Ryu M, Taguchi K, Yamamoto M, Nakazawa T	Critical role of Nrf2 in oxidative stress-induced retinal ganglion cell death.	J Neurochem	127	669-680	2013
Hayashi R, Himori N, Taguchi K, Ishikawa Y, Uesugi K, Ito M, Duncan T, Tsujikawa M, Nakazawa T, Yamamoto M, Nishida K	The role of the Nrf2-mediated defense system in corneal epithelial wound healing	Free Radic Biol Med	61	333-342	2013

別紙４

研究成果の刊行に関する一覧表（植田　弘師）

雑誌

発表者氏名	論文タイトル名	発表誌名	巻号	ページ	出版年
Halder SK, Matsunaga H, Yamaguchi H, Ueda H	Novel neuroprotective action of prothymosin α-derived peptide against retinal and brain ischemic damages	J Neurochem	125	713-723	2013
Halder SK, Sugimoto J, Matsunaga H, Ueda H	Therapeutic benefits of 9-amino acid peptide derived from prothymosin alpha against ischemic damages	Peptide	43	68-75	2013

別紙４

研究成果の刊行に関する一覧表（永井　展裕）

雑誌

発表者氏名	論文タイトル名	発表誌名	巻号	ページ	出版年
Nagai N, Kaji H, Onami H, Ishikawa Y, Nishizawa M, Osumi N, Nakazawa T, Abe T.	A polymeric device for controlled transscleral multi-drug delivery to the posterior segment of the eye	Acta Biomaterialia	10	680-687	2014

別紙４

研究成果の刊行に関する一覧表（西澤　松彦）

雑誌

発表者氏名	論文タイトル名	発表誌名	巻号	ページ	出版年
Nagai N, Kaji H, Onami H, Ishikawa Y, Nishizawa M, Osumi N, Nakazawa T, Abe T.	A polymeric device for controlled transscleral multi-drug delivery to the posterior segment of the eye	Acta Biomaterialia	10	680-687	2014

Acta Biomaterialia 10 (2014) 680–687

Contents lists available at ScienceDirect

Acta Biomaterialia

journal homepage: www.elsevier.com/locate/actabiomat

A polymeric device for controlled transscleral multi-drug delivery to the posterior segment of the eye

Nobuhiro Nagai [a], Hirokazu Kaji [b], Hideyuki Onami [a,c], Yumi Ishikawa [a], Matsuhiko Nishizawa [b], Noriko Osumi [d], Toru Nakazawa [c], Toshiaki Abe [a,*]

[a] Division of Clinical Cell Therapy, United Centers for Advanced Research and Translational Medicine (ART), Tohoku University Graduate School of Medicine, 2-1 Seiryo-machi, Aoba-ku, Sendai 980-8575, Japan
[b] Department of Bioengineering and Robotics, Graduate School of Engineering, Tohoku University, 6-6-01 Aramaki, Aoba-ku, Sendai 980-8579, Japan
[c] Department of Ophthalmology, Tohoku University Graduate School of Medicine, 1-1 Seiryo-machi, Aoba-ku, Sendai 980-8574, Japan
[d] Division of Developmental Neuroscience, United Centers for Advanced Research and Translational Medicine (ART), Tohoku University Graduate School of Medicine, 2-1 Seiryo-machi, Aoba-ku, Sendai 980-8575, Japan

ARTICLE INFO

Article history:
Received 28 August 2013
Received in revised form 26 October 2013
Accepted 8 November 2013
Available online 15 November 2013

Keywords:
Transscleral delivery
Multi-drug delivery
Retina
Poly(ethyleneglycol) dimethacrylate

ABSTRACT

The design of drug delivery systems that can deliver multiple drugs to the posterior segment of the eye is a challenging task in retinal disease treatments. We report a polymeric device for multi-drug transscleral delivery at independently controlled release rates. The device comprises a microfabricated reservoir, controlled-release cover and three different fluorescent formulations, which were made of photopolymeized tri(ethyleneglycol)dimethacrylate (TEGDM) and poly(ethyleneglycol)dimethacrylate (PEGDM). The release rate of each fluorescent is controlled by varying the PEGDM/TEGDM ratio in its formulation and the cover. The release kinetics appeared to be related to the swelling ratio of the PEGDM/TEGDM polymers. When the devices were implanted onto rat sclerae, fluorescence was observable in the ocular tissues during 4 weeks' implantation and distributed locally around the implantation site. Our polymeric system, which can administer multiple compounds with distinct kinetics, provides prolonged action and less invasive transscleral administration, and is expected to provide new tools for the treatment of posterior eye diseases with new therapeutic modalities.

1. Introduction

Diseases of the posterior eye segments cause impaired vision and blindness for millions of patients around the world [1]. There has been an increase in the understanding of the disease processes, and multiple factors have been reported to play a role in the diseases [2–4]. Thus, multi-drug therapy has become the primary method of disease management, because it offers the major advantages of enhanced efficacy of treatment, reduction of each drug dose, and mitigation of toxicity and side-effects caused by high doses of single drugs [5–7]. Multiple drugs have been used to treat patients with glaucoma [5,6] and to suppress choroidal neovascularization in patients with age-related macular degeneration (AMD) [7]. The regulation of neovascularization has received much attention, and it is now known that its balance is maintained by more than two dozen cytokines [8]. Thus it would be more effective and reasonable to use a number of drugs to treat such disease processes. Some techniques and novel pharmacological agents offer promise for the future treatment of posterior eye segment diseases [9–11]. However, the successful treatment of some retinal diseases has been limited. The limitation may be partially related to inadequate drug delivery systems for the retina, including multiple drug administration.

The principal route for local ophthalmic drug delivery remains topical application [12]. However, drug delivery to intraocular tissue by this approach is limited by the significant barrier of corneal epithelium and tear fluid turnover [13]. Systemic drug administration is not a viable alternative due to the blood–retinal barrier that limits drug access to the posterior tissues of the eye. Although intravitreal injections and intraocular implants may deliver drugs effectively to the retina and choroid, this approach is invasive to the eye and may cause severe adverse effects, such as endophthalmitis and retinal detachment [14]. Periocular or transscleral routes are less invasive than intravitreal administration and provide higher retinal and vitreal drug bioavailability (~0.01–0.1%) compared to eye drops (about 0.001% or less) [15,16]. Due to the high degree of hydration and low cell density of the sclera, soluble substrates readily pass through the sclera, although the ease of penetration of the drug to the vitreous cavity is dependent on the thickness

* Corresponding author. Tel./fax: +81 22 717 8234.
E-mail address: toshi@oph.med.tohoku.ac.jp (T. Abe).

1742-7061/$ - see front matter © 2013 Acta Materialia Inc. Published by Elsevier Ltd. All rights reserved.
http://dx.doi.org/10.1016/j.actbio.2013.11.004

of the sclera [17]. Thus transscleral delivery has the potential to be a more effective and less invasive route for intraocular drug delivery.

Several potential carriers for ocular drug delivery such as micelles [18], microneedles [19], nano- or microparticles [20,21], liposomes [22,23] and hydrogel systems [24,25] have been investigated. All the systems are injectable for localized and targeted delivery of drugs to the desired site and biodegradable to avoid a second procedure for implant removal. However, release profiles for biodegradable systems are generally complex with burst effects, i.e. an initial burst, a diffusional release phase and a final burst [26]. Additionally, the release period of such biodegradable systems is limited to less than 2 weeks [25]. In chronic eye diseases such as AMD and retinitis pigmentosa, duration of effect with controlled drug release is critical. Although several systems for multi-drug delivery have been developed [27–32], there are none intended for ocular multi-drug delivery.

In this work, we manufactured a polymeric device for multi-drug transscleral delivery to the posterior segment of the eye at independently controlled release rates (Fig. 1). The device comprises a microfabricated reservoir, controlled-release cover and drug formulations, which were made of photopolymeized tri(ethyleneglycol)dimethacrylate (TEGDM) and poly(ethyleneglycol)dimethacrylate (PEGDM). Here, we show that the release of multiple drugs can be tuned by changing the formulations of the drug as well as the covering, and demonstrate the transport of drugs into the ocular tissue in rats using fluorescents.

2. Materials and methods

2.1. Materials

PEGDM (*Mn* 750), TEGDM (*Mw* 286.3) and 2-hydroxy-2-methylpropiophenone were purchased from Aldrich (USA). Polydimethylsiloxane (PDMS), fluorescein (FL, *Mw* 332.31), rhodamine-B (Rho, *Mw* 479.02) and 4,6-diamidino-2-phenylindole dihydrochloride (DAPI, *Mw* 350.25) were purchased from Wako (Japan).

2.2. Device fabrication

The device consists of a reservoir that can contain different types of sustained release formulations and is sealed with a controlled release cover (Fig. 1c). PEGDM and TEGDM including 1% 2-hydroxy-2-methylpropiophenone as a photoinitiator were used for device materials. For the preparation of the reservoir, TEGDM prepolymer was poured into the PDMS mold fabricated via a microfabrication technique using a microprocessing machine (MicroMC-2, PMT Co.) (Supplementary Fig. S.1), and photopolymerized for 3 min with UV light (HLR400F-22, Sen Lights) at an intensity of 7.4 mW cm^{-2}. After loading the drugs, a reservoir cover was prepared by applying a prepolymer mixture of the required concentrations of PEGDM and TEGDM to the reservoir, followed by UV curing for 3 min. For the preparation of the fluorescent formulations, the fluorescents were combined with a mixture of a predetermined ratio of PEGDM and TEGDM and poured into PDMS molds and photopolymerized for 3 min. All fluorescent formulations had a fluorescent concentration of 50 mg ml^{-1} and the volume was 1.2 μl (60 μg) or 0.4 μl (20 μg) for single-fluorescent delivery or multi-fluorescent delivery devices, respectively. The dimensions of the device were 2 mm × 2 mm × 1 mm (external) and 1.55 mm × 1.55 mm × 0.5 mm (internal; maximum loading volume, 1.2 μl). PEGDM/TEGDM prepolymer mixture ratios of 100%/0%, 80%/20%, 60%/40%, 40%/60%, 20%/80% and 0%/100% were designated as P100, P80, P60, P40, P20 and P0, respectively.

2.3. Characterization of diffusion mechanism through the PEGDM/TEGDM system

The permeability of FL in phosphate-buffered saline (PBS) (0.5 mg ml^{-1}, 20 μl) through the PEGDM/TEGDM reservoir (4 mm × 4 mm × 1.5 mm, internal) was assessed by monitoring the increase in fluorescence in the external PBS (1 ml) solution with time ($n = 5$). To characterize the diffusion mechanism through the PEGDM/TEGDM system, we determined the swelling ability of the PEGDM/TEGDM polymers. The samples (size: 5 mm × 5 mm × 2 mm) with various PEGDM/TEGDM ratios were weighed in air before (W_b) and after (W_a) immersion for 24 h in 10 ml of PBS, and the swelling ratio ($W_a/W_b \times 100$) was calculated ($n = 5$).

2.4. In vitro release study

For the single delivery study, FL was pelletized with P60 and loaded in the device, followed by sealing with P100, P60 or P40 covers. For the multiple delivery, three types of fluorescents, FL, Rho and DAPI, were pelletized each with different ratios of PEGDM/TEGDM and loaded in the device, followed by sealing with P100 or P60 covers. The devices were each incubated in 1 ml of PBS at 37 °C. To estimate the amounts of fluorescent that had diffused out of the devices, the fluorescence intensities of the PBS solutions

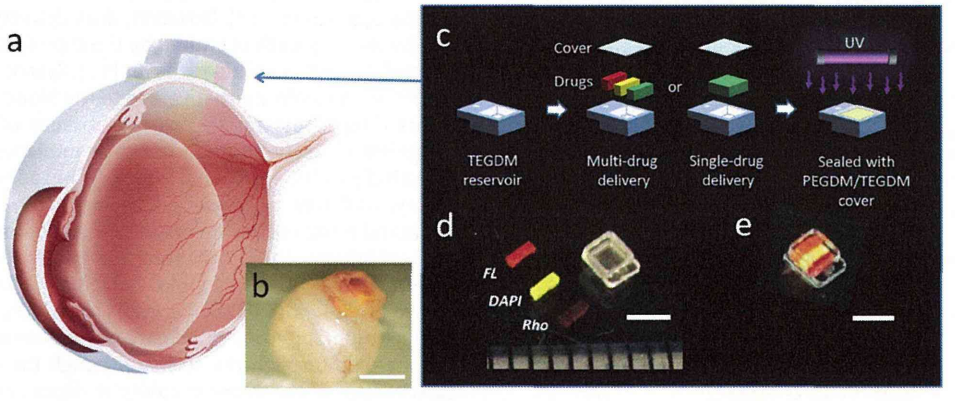

Fig. 1. (a) Schematic image of transscleral intraocular multi-drug delivery using a polymeric device placed on the sclera. (b) Photograph of the rat eye where the device was implanted on the sclera for 3 days. (c) Image shows assembling process of the device that consists of three kinds of fluorescents pelletized with PEGDM/TEGDM, a reservoir made of TEGDM and a controlled release cover made of PEGDM/TEGDM. After loading the pellets in the reservoir, the cover was sealed on the reservoir by UV curing. (d) Photographs showing three kinds of fluorescent pellets, including FL, Rho and DAPI, and a reservoir before assembling, and (e) the device after assembling. Scale bars, 2 mm.

were measured spectrofluorometrically (FluoroscanAscent; Thermo), where fluorescence excitation (ex) and emission (em) for FL, Rho and DAPI was measured at ex. 485 nm/em. 538 nm, ex. 544 nm/em. 590 nm and ex. 355 nm/em. 460 nm, respectively ($n = 6$). The PBS was replenished during the course of the release study to ensure that the concentration of fluorescent molecules was below 20% of its saturation value at all times. The results were expressed as amount determined using a standard curve.

2.5. Animal experiments

Male Sprague–Dawley rats (SLC) weighing 250–300 g were used in this study. All animals were handled in accordance with the Association for Research in Vision and Ophthalmology Statement for the Use of Animals in Ophthalmic and Vision Research after receiving approval from the Institutional Animal Care and Use Committee of the Tohoku University Environmental & Safety Committee (No. 2013MdA-218).

2.6. Implantation

The rats were anesthetized with ketamine hydrochloride (90 mg kg^{-1}) and xylazine hydrochloride (10 mg kg^{-1}). Their ocular surfaces were anesthetized with a topical instillation of 0.4% oxybuprocaine hydrochloride. A paralimbal conjunctival incision was made 1 mm from the temporal limbus. The devices were placed onto the left eyes at the sclerae. The right eyes served as controls.

2.7. In vivo release study

After implantation, the eyes were enucleated and the conjunctiva, muscle, optic nerve and the device were carefully removed. Fluorescent images were captured using a hand-held retinal camera for fluorescein angiography (Genesis-D, Kowa) to document the fluorescence distributions around the implantation site. After taking the image, the eyes were carefully separated into the retina, vitreous, lens, cornea and sclera/choroid/retinal pigment epithelium (RPE). The retina and sclera/choroid/RPE were homogenized in 100 μl of lysis buffer (1% Triton X-100 in PBS). The homogenates were centrifuged at 15,000g for 10 min, and the fluorescence intensity of the 80 μl of supernatant was measured spectrofluorometrically (FluoroscanAscent) ($n = 6$). For histological examination, the eyes were frozen in liquid nitrogen. A suture was placed as a landmark at the implant site of the device. After mounting the cryostat sections in a medium (Vectashield, Vector Lab), the distribution of fluorescein was observed by fluorescent microscopy (DMI6000B, Leica).

2.8. Statistical analysis

Experimental data are presented as means ± standard deviations (SD). Statistical significance was calculated with Ekuseru-Toukei 2012 (Social Survey Research Information), using the unpaired t-test for normally distributed isolated pairs, and the analysis of variance (ANOVA) with Tukey's test for multiple comparisons. Differences were considered significant if $p < 0.05$ (*).

3. Results

3.1. Device fabrication

The device consists of a separately fabricated TEGDM reservoir, fluorescent formulations and a PEGDM/TEGDM cover (Fig. 1c). The device was designed to deliver various formulations and dosages. In this study, sustained-release fluorescent formulations, including a single FL pellet or multiple FL/Rho/DAPI pellets (Fig. 1d), were encapsulated in the reservoir using a cover to prolong fluorescent release by limiting the rate of fluorescent dissolution within the reservoir. After loading the fluorescent pellets, the PEGDM/TEGDM prepolymer was cast over the reservoir and UV-cured to provide a seal (Fig. 1e). Because photopolymerized TEGDM is impermeable to small molecules (see below), the reservoir is a barrier that forces unidirectional fluorescent release to the sclera side.

3.2. Diffusion mechanism through the PEGDM/TEGDM system

Fig. 2a shows that the release of FL was dependent on the PEGDM/TEGDM ratio. Pure PEGDM (P100) shows the highest permeability, whereas pure TEGDM (P0) was impermeable. The release rate estimated from the slope of the curve at the initial linear state was 1296 (P100), 684 (P80), 333 (P60), 83 (P40), 35 (P20) and 0 (P0) ng day^{-1}. The release rate gradually decreased as the cumulative release approached the plateau level (10 μg ml^{-1}, maximum concentration when FL was fully released in PBS), as was seen in P100 and P80. Fig. 2b shows that the swelling ratio increased with increasing the PEGDM ratio. Fig. 2c shows the correlation of the swelling ratio, obtained from the results in Fig. 2b, with the slope obtained from the release profile results in Fig. 2a. The correlation coefficient was 0.9904, indicating almost linear correlation between the swelling ratio and release rate.

3.3. Single FL release study

Fig. 3a shows the single release profiles of FL-loaded devices that were sealed with different types of covers. Although FL-pellets without reservoir or cover showed a rapid burst-like release over 5 days, the covered devices showed a zero-order release without an initial burst. The release rate decreased with decreasing PEGDM ratio in the cover. The release rate estimated from the gradient curve for pellet, P100-, P60- and P40-covered devices were 20.7, 1.13, 0.53 and 0.10 μg day^{-1}, respectively. The results demonstrate the ability to control the release rate from a device by changing the ratio of PEGDM/TEGDM in the cover.

Devices containing FL pellet (F60) and sealed with P100, P60 and P40 covers, and pellets without reservoir or cover, were implanted onto the sclerae of rats. The devices remained at the implantation site during the experiments and were easily removed from the implantation site at the end of experiments. Routine ophthalmological examinations showed no device-related toxic effects. To demonstrate the controllability of the in vivo release of FL, images of fluorescence in the sclera after removing the device were captured by a hand-held camera (Fig. 3b). White areas corresponding to fluorescence indicate the distribution of released FL. For the pellet only, little fluorescence was observed at 1 week after implantation, probably due to the burst-like release within 5 days. For the P100-cover devices, the intensity was high at 1 week, then decreased gradually during the subsequent 3 weeks. For the P60-cover devices, the intensity was moderate for 2 weeks, then weak intensity was sustained during the remaining 2 weeks. For the P40-cover devices, weak fluorescence was sustained during 4 weeks. Trends in the fluorescence intensity were almost comparable to the in vitro release results (Fig. 3a).

Fig. 4a–d shows sectional images of an eye around the implantation site. FL (green areas) penetrated the sclera at least 1 day after implantation (Fig. 4a and c), and then reached the choroid/RPE at least 3 days after implantation (Fig. 4b and d). Intense fluorescent can be seen at the RPE, one of the blood–retinal barriers (Fig. 4d). Blurred fluorescent that passed through the RPE can be seen at the retina, indicating the passing of the molecules through the RPE into the neural retina. The amount of FL in the

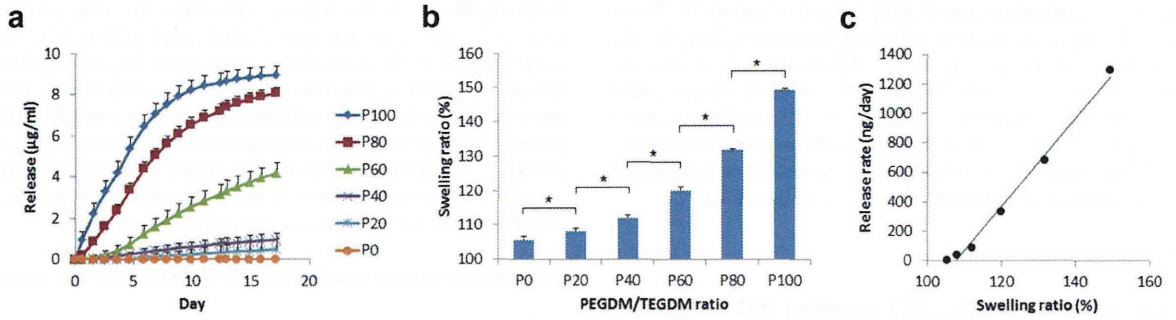

Fig. 2. (a) Permeability of FL in PBS through the PEGDM/TEGDM reservoir with various PEGDM/TEGDM ratios. The release was assessed by monitoring the increase in fluorescence in the external PBS solution with time. (b) Swelling ability in PBS of PEGDM/TEGDM polymers (size: 5 mm × 5 mm × 2 mm) with various PEGDM/TEGDM ratios. (c) Correlation between swelling ratio in (b) and release rate. Release rate was estimated from the slope of the curve of the line at the initial stable release period in (a). Values are mean ± SD. $*p < 0.05$ (one-way analysis of variance (ANOVA) with Tukey's test).

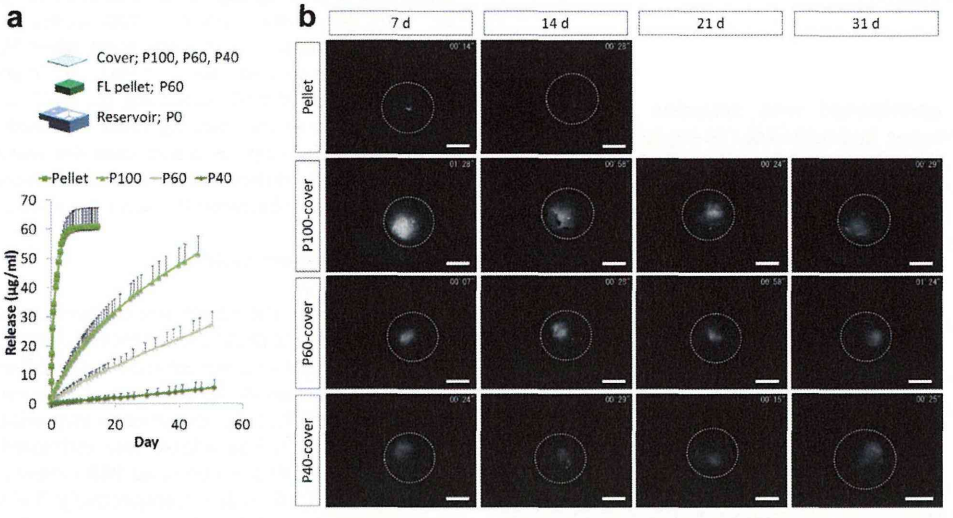

Fig. 3. (a) Release profiles of a single-drug delivery device that consists of a FL formulation pelletized with P60 and various types of cover (P100, P60 and P40), and FL pellet with no reservoir or cover. FL release was monitored spectrofluorometrically. (b) Fluorescent images of the sclera after removing the devices. Devices were implanted on the sclerae in rats for 7, 14, 21 and 31 days. White areas show released FL and circular dotted lines show the shape of the eyeball. Values are mean ± SD. Scale bars: 2 mm.

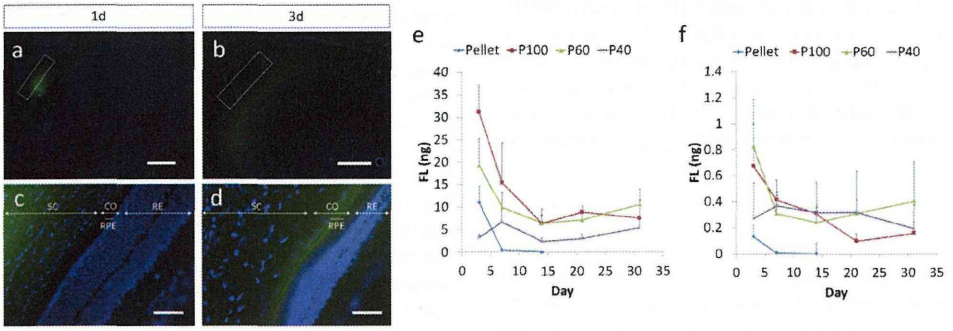

Fig. 4. The distribution of FL (green) in the retina and sclera around the implantation site (a, c) 1 day and (b, d) 3 days after implantation (square dots: device implantation site). Cell nuclei were stained with DAPI (blue). FL accumulated at RPE by day 3 after implantation and a portion of FL penetrated through the RPE and reached the retina. The amounts of FL in the sclera/choroid/RPE (e) and retinal fractions (f) during 1 month implantation. Abbreviations: sclera (SC), retinal pigment epithelium (RPE), choroid (CO) and retina (RE). Scale bars: 1 mm (a, b), 100 μm (c, d). Values are mean ± SD.

sclera/choroid/RPE, and retinal fractions during 4 weeks' implantation was measured. For the sclera/choroid/RPE fraction (Fig. 4e), the amount of FL correlated with the release profiles of the covered devices at the first week (P100 > P60 > P40). Pellet only showed almost no fluorescence after 1 week due to the burst-like release within 5 days, as is seen in Fig. 3a. From 2 weeks' implantation onwards, the amounts of FL for the P100- and P60-covered devices were at almost the same level, whereas the amount for the P40-covered device was consistently at a lower level during the successive incubation. These results are well matched with the fluorescent images on the sclera shown in Fig. 3b. For the retinal fraction (Fig. 4f), the amount of FL differed among the devices

for the first week, but was then maintained at almost the same level for each device during the following 2 weeks. Pellet only was unable to deliver FL to the retina except during the early days. After 3 weeks, the FL level for the P100-covered device was lower, while the level for the P40-covered device had decreased after 4 weeks. Although the amount of FL in the retina shows little correlation with the release profiles, the results demonstrate that fluorescent molecules released from the devices could reach the retina during the 4 weeks of implantation and the amount of FL was reduced to between 1/30 and 1/40 at the retina after passing through the sclera.

3.4. Multiple FL/Rho/DAPI release study

The simultaneous independently controlled multiple release was tested using three kinds of fluorescents, FL, Rho, and DAPI, which may mimic low-molecular-weight drugs. The device was filled with three kinds of pellets, each with different ratios of PEGDM/TEGDM. The release profiles of each pellet are shown in Supplementary Fig. S.2. DAPI pelletized with P100 (D100) was always included in the device as a constant control. FL was pelletized with P100 (F100), P70 (F70) and P60 (F60). Rho was also pelletized with P100 (R100), P70 (R70) and P60 (R60). Fig. 5a–c shows that the release rate of the molecules can be tuned by changing the composition of each pellet. For example, the release rate of FL or Rho varied as the PEGDM ratio changed (Fig. 5a vs. Fig. 5b), whereas that of DAPI was constant. When the device was sealed with a P60 cover, the absolute amount released decreased to between one-fourth and one-eighth in all of the devices compared to the P100-covered devices, but importantly, the ability to independently control the release rates of the molecules was maintained (Fig. 5d–f). If the release results were sorted for each molecule, the release kinetics of each molecule was always dependent on the PEGDM/TEGDM ratio of the pellet (Supplementary Fig. S.3). These results indicate that the release kinetics can be tuned via two independent diffusion mechanisms afforded by a sustained-release formulation and a controlled release cover.

Devices containing a combination of F60/R40/D60 pellets (device A) or F60/R60/D40 pellets (device B), sealed with a P60 cover, were implanted onto the rat sclerae. Fig. 6a–h shows the sectional images for 1 and 4 weeks after implantation. Magnified images showed fluorescence at the outer nuclear layer (ONL) in the retina and the intensity of the fluorescence correlates with device condition; device A, which releases DAPI at a faster rate than device B, shows more intense blue fluorescence in the ONL compared with device B (Fig. 6b and f). On the other hand, device B, which releases Rho at a faster rate than device A, exhibits more red fluorescence in the retina than that of device A (Fig. 6d and h). Low magnification images of the sections showed the local distribution of released fluorescents around the implantation site 1 and even 4 weeks after implantation (Fig. 6a, c, e and g). This may indicate that the released drug is specifically delivered to the retina local to the implantation site.

The amounts of fluorescence in the sclera/choroid/RPE (Fig. 7a–c) and the retina fractions (Fig. 7d–f) at 1, 2 and 4 weeks after implantation were measured. Because FL was set to release at the same rate in each device, there was no significant difference between the amount of FL detected in the fractions for device A or B (Fig. 7a and d). On the other hand, the amount of Rho in sclera/choroid/RPE and retinal fractions for device B was higher than for device A, and at 4 weeks' implantation a significant difference (p value: 0.042) can be seen in the sclera/choroid/RPE fraction (Fig. 7b). Similarly, the amount of DAPI for device A was significantly higher than for device B at 4 weeks' implantation (p value; 0.037) (Fig. 7c). There was no difference between Rho and DAPI intensities in the retina for the devices (Fig. 7e and f).

4. Discussion

We established a transscleral multi-drug delivery device with which we demonstrated the transport of low-molecular-weight compounds into the ocular tissue using fluorescents. The release of multiple drugs can be tuned by changing the formulations of the drug as well as the covering. The ability to control the release of fluorescents from the PEGDM/TEGDM system may be explained by the results of swelling tests (Fig. 2). The polymers made of short chains of TEGDM are likely to be compact, with little ability to swell, and impermeable to low-molecular-weight compounds. On the other hand, long chains of PEGDM may result in more open polymer networks, showing a greater tendency to swell, facilitating permeation of small molecules. Further, the release rate of each fluorescent differs, even when we used the same pelletized

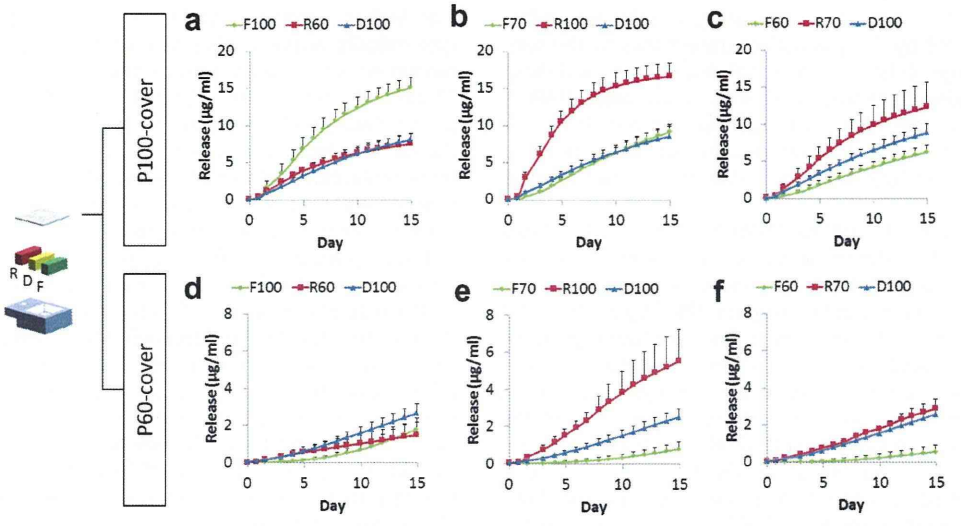

Fig. 5. (a–f) Release profiles of a multi-drug delivery device that consists of three types of fluorescent pellets (FL, Rho and DAPI, designated F, R and D, respectively, in the schematic) made of various PEGDM/TEGDM content, and two types of cover (P100 cover: (a–c), P60 cover: (d–f)). DAPI was pelletized with P100 as a constant release control. FL and Rho were pelletized with P100, P70 and P60, respectively. Values are mean ± SD.

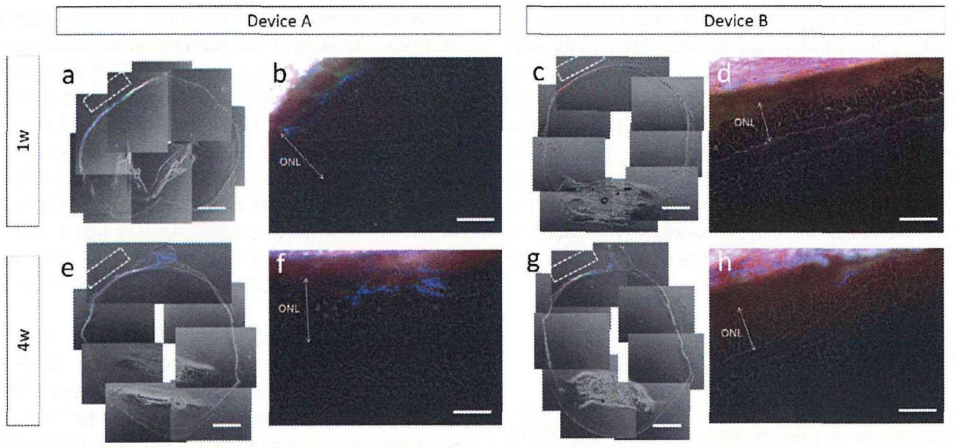

Fig. 6. (a–h) The distribution of FL (green), Rho (red) and DAPI (blue) in the retina and sclera around the implantation site 1 week (a–d) and 4 weeks (e–h) after implantation (square dots: device implantation site). Two types of devices, device A (F60/R40/D60) and B (F60/R60/D40), were used. Device A shows faster DAPI release than Rho and device B shows faster Rho release than DAPI. Magnified images (b, d, f, h) show that fluorescents reached the outer nuclear layer (ONL, double-headed allows). Scale bars, 1 mm (a, c, e, g) and 100 μm (b, d, f, h).

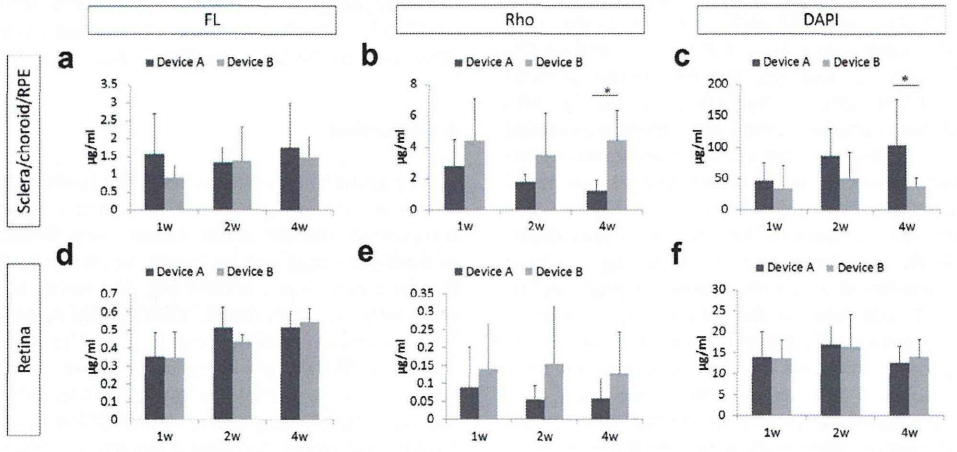

Fig. 7. The amounts of FL, Rho and DAPI in the sclera/choroid/RPE (a–c) and retinal fractions (d–f) during 4 weeks' implantation. Values are mean ± SD. $^{*}p < 0.05$ (unpaired *t*-test for normally distributed isolated pairs).

conditions (Supplementary Fig. S.2), indicating that the permeability may be influenced by the physical characteristics of the substance, such as lipophilicity, water solubility and acid–base character; FL and Rho-B are weak carboxylic acids, while DAPI is a base [33]. Therefore, we need to consider the physical characteristics of the substances and their interactions when determining the optimum PEGDM/TEGDM system for the intended drug release.

The device materials, PEGDM and TEGDM, are bio-inert and can be easily molded into different substrate shapes by UV curing [34,35]. We used a microfabrication technique because the shape and volume of the reservoir can be easily modified by an AutoCAD design. We have previously reported a reservoir-based protein-drug-release device sealed with a PEGDM cover including collagen microparticles, which served as permeation porogen for macromolecules [36]. We found that low-molecular-weight molecules can easily pass through polymerized PEGDM membrane, whereas polymerized TEGDM is impermeable to them (Fig. 2). Therefore, we newly developed a controlled release system for low-molecular-weight drugs using a PEGDM/TEGDM mixture. Some monomers of unpolymerized PEGDM and TEGDM and photoinitiator were found to elute from the device, but the amount of elution (the highest amount is 504 ng ml^{-1}) was significantly less than cytotoxically active levels (more than 391 μg ml^{-1}), and no more monomers and photoinitiator eluted after incubation in PBS for 15 days (Supplementary Fig. S.4). The PEGDM/TEGDM polymer shows almost no biodegradation 19 months after implantation on the rabbit sclera (Supplementary Fig. S.5). Additionally, the long-term implantation of the device over 4 weeks did not affect retinal function assessed by electroretinograms (Supplementary Fig. S.6). Thus, the device would appear to be stable and biocompatible for at least 1 year, and can be used to safely administer drugs by the transscleral approach without disturbing intraocular tissues.

Fluorescents were used for the analysis of drug transport into the eye from the device. Although fluorescence was observable in the ocular tissues during 4 weeks' implantation and distributed locally around the implantation site, the fluorescein concentration in the retina seemed to be almost the same in spite of the difference in the release profiles of the devices (Figs. 4f and 7e and f). This may be due to the blood–retinal barrier restricting drug transport through the RPE to the retina. Pitkanen reported that the permeability through the RPE depended on the lipophilicity and molecular weight of drugs [37]. Additionally, transporters in the RPE probably have a greater role in ocular pharmacokinetics [38]. In

fact, we observed FL accumulation around the RPE (Fig. 4d), indicating that the drug transport was restricted here. This may be one of the reasons for the constant amount of fluorescents in the retina. Additionally, this behavior might be due to the availability of fluorescents at the retina, because transport and penetration through the sclera, choroid and RPE may vary between molecules [37]. The clearance rate by blood vessels may also be different for hydrophobic and hydrophilic molecules [15]. Our device has a low-molecular-weight-impermeable reservoir that can release drugs unidirectionally to the sclera, making it less susceptible to drug elimination by conjunctival lymphatic/blood vessel clearance, so the choroid may be the primary route of clearance. Further study is needed to elucidate the factors influencing drug availability to the retina. Given that the distribution of fluorescents was concentrated at the RPE and adjacent regions, our device may be effective, especially for lesions in the vicinity of the RPE.

One of the limitations of this study is the lack of a study proving retinal neuroprotective effects of our device using clinical drugs. Previous reports show potent effective drugs, such as edaravone [39], geranylgeranylaceton [40] and unoprostone [41] against retinal degeneration in animals, whereas these drugs are administered via systemic route, topical eye drop or intravitreal injection. We are planning to perform an animal study using the clinical drugs to investigate the efficacy of our controlled transscleral multi-drug delivery system on retinal neuroprotection.

5. Conclusion

A polymeric system which can administer multiple compounds with distinct kinetics to the posterior segment of the eye was manufactured. The release of multiple compounds can be tuned by changing their formulations as well as the device covering. Furthermore, our system can be used to safely administer drugs by the transscleral approach without disturbing intraocular tissues. Strict local delivery of the drugs through our device may facilitate the administration of the drugs that would not be suitable for systemic use due to side-effects. Additionally, prolonged sustained drug release using our device would be suitable for the treatment of chronic retinal diseases. Thus, our polymeric system provides prolonged action and less invasive intraocular administration, and is expected to provide new tools for the treatment of posterior eye diseases with new therapeutic modalities.

Competing financial interests

The authors declare no conflict of interest.

Acknowledgements

This study was supported by Grant-in-Aid for Young Scientists (A) from the Ministry of Education, Culture, Sports, Science, and Technology 23680054 (N.N.), Health Labour Sciences Research Grant from the Ministry of Health Labour and Welfare H23-iryokiki-wakate-003 (N.N.), H23-kankaku-ippan-004 (T.A. and N.N.), H24-nanchitoh-ippan-067 (T.A. and N.N.), the Takeda Science Foundation (N.N.), the Tohoku University Exploratory Research Program for Young Scientists (N.N.) and Gonryo Medical Foundation (N.N.). We thank T. Kawashima, N. Kumasaka, T. Yamada and S. Ito for help with device molds preparation.

Appendix A. Supplementary data

Supplementary data associated with this article can be found, in the online version, at http://dx.doi.org/10.1016/j.actbio.2013.11.004.

References

[1] Resnikoff S, Pascolini D, Etya'ale D, Kocur I, Pararajasegaram R, Pokharel GP, et al. Global data on visual impairment in the year 2002. Bull World Health Organ 2004;82:844–51.
[2] Gragoudas ES, Adamis AP, Cunningham Jr ET, Feinsod M, Guyer DR. Pegaptanib for neovascular age-related macular degeneration. N Engl J Med 2004;351:2805–16.
[3] Kim M, Yoon BJ. Adaptive reference update (ARU) algorithm. A stochastic search algorithm for efficient optimization of multi-drug cocktails. BMC Genomics 2012;13(Suppl 6):S12.
[4] Calkins DJ. Critical pathogenic events underlying progression of neurodegeneration in glaucoma. Prog Retin Eye Res 2012;31:702–19.
[5] Fu QL, Li X, Yip HK, Shao Z, Wu W, Mi S, et al. Combined effect of brain-derived neurotrophic factor and LINGO-1 fusion protein on long-term survival of retinal ganglion cells in chronic glaucoma. Neuroscience 2009;162:375–82.
[6] Shin DH, Feldman RM, Sheu WP. Efficacy and safety of the fixed combinations latanoprost/timolol versus dorzolamide/timolol in patients with elevated intraocular pressure. Ophthalmology 2004;111:276–82.
[7] Spaide RF. Rationale for combination therapy in age-related macular degeneration. Retina 2009;29:S5–7.
[8] He S, Xia T, Wang H, Wei L, Luo X, Li X. Multiple release of polyplexes of plasmids VEGF and bFGF from electrospun fibrous scaffolds towards regeneration of mature blood vessels. Acta Biomater 2012;8:2659–69.
[9] Campochiaro PA. Potential applications for RNAi to probe pathogenesis and develop new treatments for ocular disorders. Gene Ther 2006;13:559–62.
[10] Frasson M, Picaud S, Leveillard T, Simonutti M, Mohand-Said S, Dreyfus H, et al. Glial cell line-derived neurotrophic factor induces histologic and functional protection of rod photoreceptors in the rd/rd mouse. Invest Ophthalmol Vis Sci 1999;40:2724–34.
[11] Rosenfeld PJ, Brown DM, Heier JS, Boyer DS, Kaiser PK, Chung CY, et al. Ranibizumab for neovascular age-related macular degeneration. N Engl J Med 2006;355:1419–31.
[12] Hughes PM, Olejnik O, Chang-Lin JE, Wilson CG. Topical and systemic drug delivery to the posterior segments. Adv Drug Deliv Rev 2005;57:2010–32.
[13] Del Amo EM, Urtti A. Current and future ophthalmic drug delivery systems. A shift to the posterior segment. Drug Discov Today 2008;13:135–43.
[14] Geroski DH, Edelhauser HF. Transscleral drug delivery for posterior segment disease. Adv Drug Deliv Rev 2001;52:37–48.
[15] Ranta VP, Urtti A. Transscleral drug delivery to the posterior eye: prospects of pharmacokinetic modeling. Adv Drug Deliv Rev 2006;58:1164–81.
[16] Ambati J, Adamis AP. Transscleral drug delivery to the retina and choroid. Prog Retin Eye Res 2002;21:145–51.
[17] Olsen TW, Edelhauser HF, Lim JI, Geroski DH. Human scleral permeability. Effects of age, cryotherapy, transscleral diode laser, and surgical thinning. Invest Ophthalmol Vis Sci 1995;36:1893–903.
[18] Li X, Zhang Z, Li J, Sun S, Weng Y, Chen H. Diclofenac/biodegradable polymer micelles for ocular applications. Nanoscale 2012;4:4667–73.
[19] Patel SR, Berezovsky DE, McCarey BE, Zarnitsyn V, Edelhauser HF, Prausnitz MR. Targeted administration into the suprachoroidal space using a microneedle for drug delivery to the posterior segment of the eye. Invest Ophthalmol Vis Sci 2012;53:4433–41.
[20] Aksungur P, Demirbilek M, Denkbas EB, Vandervoort J, Ludwig A, Unlu N. Development and characterization of Cyclosporine A loaded nanoparticles for ocular drug delivery: cellular toxicity, uptake, and kinetic studies. J Control Release 2011;151:286–94.
[21] Chhablani J, Nieto A, Hou H, Wu EC, Freeman WR, Sailor MJ, et al. Oxidized porous silicon particles covalently grafted with daunorubicin as a sustained intraocular drug delivery system. Invest Ophthalmol Vis Sci 2013;54:1268–79.
[22] Chen CW, Lu DW, Yeh MK, Shiau CY, Chiang CH. Novel RGD-lipid conjugate-modified liposomes for enhancing siRNA delivery in human retinal pigment epithelial cells. Int J Nanomedicine 2011;6:2567–80.
[23] Kaiser JM, Imai H, Haakenson JK, Brucklacher RM, Fox TE, Shanmugavelandy SS, et al. Nanoliposomal minocycline for ocular drug delivery. Nanomedicine 2013;9:130–40.
[24] Li X, Zhang Z, Chen H. Development and evaluation of fast forming nano-composite hydrogel for ocular delivery of diclofenac. Int J Pharm 2013;448:96–100.
[25] Wang CH, Hwang YS, Chiang PR, Shen CR, Hong WH, Hsiue GH. Extended release of bevacizumab by thermosensitive biodegradable and biocompatible hydrogel. Biomacromolecules 2012;13:40–8.
[26] Kunou N, Ogura Y, Yasukawa T, Kimura H, Miyamoto H, Honda Y, et al. Long-term sustained release of ganciclovir from biodegradable scleral implant for the treatment of cytomegalovirus retinitis. J Control Release 2000;68:263–71.
[27] Zhang H, Zhao C, Cao H, Wang G, Song L, Niu G, et al. Hyperbranched poly(amine-ester) based hydrogels for controlled multi-drug release in combination chemotherapy. Biomaterials 2010;31:5445–54.
[28] Shin HC, Alani AW, Rao DA, Rockich NC, Kwon GS. Multi-drug loaded polymeric micelles for simultaneous delivery of poorly soluble anticancer drugs. J Control Release 2009;140:294–300.
[29] Richardson TP, Peters MC, Ennett AB, Mooney DJ. Polymeric system for dual growth factor delivery. Nat Biotechnol 2001;19:1029–34.
[30] Lammers T, Subr V, Ulbrich K, Peschke P, Huber PE, Hennink WE, et al. Simultaneous delivery of doxorubicin and gemcitabine to tumors in vivo using prototypic polymeric drug carriers. Biomaterials 2009;30:3466–75.

[31] Elia R, Fuegy PW, VanDelden A, Firpo MA, Prestwich GD, Peattie RA. Stimulation of in vivo angiogenesis by in situ crosslinked, dual growth factor-loaded, glycosaminoglycan hydrogels. Biomaterials 2010;31:4630–8.
[32] Wang Y, Wang B, Qiao W, Yin T. A novel controlled release drug delivery system for multiple drugs based on electrospun nanofibers containing nanoparticles. J Pharm Sci 2010;99:4805–11.
[33] Dickens SH, Flaim GM, Floyd CJ. Effects of adhesive, base and diluent monomers on water sorption and conversion of experimental resins. Dent Mater 2010;26:675–81.
[34] Benoit DS, Durney AR, Anseth KS. Manipulations in hydrogel degradation behavior enhance osteoblast function and mineralized tissue formation. Tissue Eng 2006;12:1663–73.
[35] Kalachandra S. Influence of fillers on the water sorption of composites. Dent Mater 1989;5:283–8.
[36] Kawashima T, Nagai N, Kaji H, Kumasaka N, Onami H, Ishikawa Y, et al. A scalable controlled-release device for transscleral drug delivery to the retina. Biomaterials 2011;32:1950–6.
[37] Pitkanen L, Ranta VP, Moilanen H, Urtti A. Permeability of retinal pigment epithelium: effects of permeant molecular weight and lipophilicity. Invest Ophthalmol Vis Sci 2005;46:641–6.
[38] Mannermaa E, Vellonen KS, Urtti A. Drug transport in corneal epithelium and blood-retina barrier: emerging role of transporters in ocular pharmacokinetics. Adv Drug Deliv Rev 2006;58:1136–63.
[39] Imai S, Inokuchi Y, Nakamura S, Tsuruma K, Shimazawa M, Hara H. Systemic administration of a free radical scavenger, edaravone, protects against light-induced photoreceptor degeneration in the mouse retina. Eur J Pharmacol 2010;642:77–85.
[40] Tanito M, Kwon YW, Kondo N, Bai J, Masutani H, Nakamura H, et al. Cytoprotective effects of geranylgeranylacetone against retinal photooxidative damage. J Neurosci 2005;25:2396–404.
[41] Tsuruma K, Tanaka Y, Shimazawa M, Mashima Y, Hara H. Unoprostone reduces oxidative stress- and light-induced retinal cell death, and phagocytotic dysfunction, by activating BK channels. Mol Vis 2011;17:3556–65.

Combined 25-Gauge Microincision Vitrectomy and Toric Intraocular Lens Implantation With Posterior Capsulotomy

Hiroshi Kunikata, MD, PhD; Naoko Aizawa, MD; Yasuhiko Meguro, MD; Toshiaki Abe, MD, PhD; Toru Nakazawa, MD, PhD

PURPOSE: To evaluate the efficacy of combined 25-gauge microincision vitrectomy surgery (MIVS) and toric intraocular lens (IOL) implantation with posterior capsulotomy.

METHODS: Noncomparative, interventional case series performed at a single center. Twelve patients with vitreoretinal disease and cataracts, with pre-existing regular corneal astigmatism greater than 1 diopter, underwent 25-gauge MIVS and toric IOL implantation with posterior capsulotomy.

RESULTS: The toric IOL was successfully implanted in each case. At 6 months postoperatively, mean axis rotation was 5.7° ± 3.1°. At 1 month postoperatively, mean uncorrected and best corrected visual acuity improved; the improvement was maintained after 6 months. The absolute residual refractive cylinder was significantly lower postoperatively than the pre-existing regular corneal cylinder (P = .003). There were no surgical complications except a temporary posterior irissynechia in one case.

CONCLUSIONS: Combined 25-gauge MIVS and toric IOL implantation with posterior capsulotomy is a practical and safe method to treat vitreoretinal disease and cataracts with pre-existing corneal astigmatism.

[*Ophthalmic Surg Lasers Imaging Retina.* **2013;44:XX-XX.**]

INTRODUCTION

Recent advanced sutureless vitrectomy techniques have hastened visual recovery, with reduction in postoperative astigmatism, conjunctival injection, pain, and discomfort.[1-7] The correction of refractive errors, including corneal astigmatism, has thus become a consideration in vitrectomy combined with cataract surgery. Toric intraocular lenses (IOLs) have been implanted in patients worldwide, and their feasibility has been demonstrated.[8-10] Over 30% of eyes indicated for cataract surgery have corneal astigmatism of at least 1.00 diopter (D).[11] Nevertheless, because of the technical difficulty of vitreous surgery and the emphasis on retinal disease control, toric IOLs have not been combined with vitrectomy surgery.

Twenty-five-gauge microincision vitrectomy surgery (25G MIVS) was first reported in 2002, and this technique is commonly used throughout the world.[12,13] Some patients (fewer than 1%) should forego MIVS or only undergo it with caution;[14] however, the indications for 25G MIVS have expanded to diseases including proliferative diabetic retinopathy (PDR), rhegmatogenous retinal detachment, giant retinal tear, intraocular foreign body, and IOL dislocation.[15-25] The increase in popularity of 25G MIVS has been enhanced by studies that have demonstrated its advantages for postoperative quality of vision. This is because intraoperative suturing is not required.[1-7] Recently, to prevent postoperative posterior capsule opacification (PCO) in patients with vitreoretinal disease who must have a vitrectomy combined with cataract surgery, a primary posterior capsulotomy technique using a 25-gauge vitreous cutter has been

From the Department of Ophthalmology, Tohoku University Graduate School of Medicine, Sendai, Japan (HK, NA, YM, TN); and the Division of Clinical Cell Therapy, Tohoku University Graduate School of Medicine, Sendai, Japan (TA).

Presented at the Sendai Toric IOL Conference, November 3, 2011.

The authors have no financial or proprietary interest in the materials presented herein.

Address correspondence to Hiroshi Kunikata, MD, Department of Ophthalmology, Tohoku University Graduate School of Medicine, 1-1 Seiryo-machi, Aoba-ku, Sendai 980-8574, Japan; +81 22 717 7294, Fax: +81 22 717 7298; Email: kunikata@oph.med.tohoku.ac.jp.

doi: